Pitfalls in the n-mode representation of vibrational potentials



Emily L. Yang [6]; Justin J. Talbot [6]; Ryan J. Spencer [6]; Ryan P. Steele [5]



J. Chem. Phys. 159, 204104 (2023) https://doi.org/10.1063/5.0176612







The Journal of Chemical Physics

Special Topic: Algorithms and Software for Open Quantum System Dynamics

Submit Today





Pitfalls in the *n*-mode representation of vibrational potentials

Cite as: J. Chem. Phys. 159, 204104 (2023); doi: 10.1063/5.0176612 Submitted: 15 September 2023 • Accepted: 19 October 2023 •

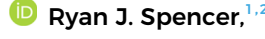








Published Online: 27 November 2023







AFFILIATIONS

- Department of Chemistry, The University of Utah, 315 S 1400 E, Salt Lake City, Utah 84112, USA
- ²Henry Eyring Center for Theoretical Chemistry, The University of Utah, Salt Lake City, Utah 84112, USA
- Department of Chemistry, University of California-Berkeley, 420 Latimer Hall, Berkeley, California 94720, USA

ABSTRACT

Simulations of anharmonic vibrational motion rely on computationally expedient representations of the governing potential energy surface. The n-mode representation (n-MR)—effectively a many-body expansion in the space of molecular vibrations—is a general and efficient approach that is often used for this purpose in vibrational self-consistent field (VSCF) calculations and correlated analogues thereof. In the present analysis, a lack of convergence in many VSCF calculations is shown to originate from negative and unbound potentials at truncated orders of the n-MR expansion. For cases of strong anharmonic coupling between modes, the n-MR can both dip below the true global minimum of the potential surface and lead to effective single-mode potentials in VSCF that do not correspond to bound vibrational problems, even for bound total potentials. The present analysis serves mainly as a pathology report of this issue. Furthermore, this insight into the origin of VSCF non-convergence provides a simple, albeit ad hoc, route to correct the problem by "painting in" the full representation of groups of modes that exhibit these negative potentials at little additional computational cost. Somewhat surprisingly, this approach also reasonably approximates the results of the next-higher n-MR order and identifies groups of modes with particularly strong coupling. The method is shown to identify and correct problematic triples of modes—and restore SCF convergence—in two-mode representations of challenging test systems, including the water dimer and trimer, as well as protonated tropine.

Published under an exclusive license by AIP Publishing. https://doi.org/10.1063/5.0176612

I. INTRODUCTION

Recent advances in cold-ion sources and tandem mass spectrometry-based spectroscopies have yielded critical insights into the fundamental nature of intermolecular interactions in molecular clusters and ions. 1-10 Interpretation of these modern vibrational spectroscopy experiments now routinely relies on close collaborations between experiment and theory. For cases of particularly influential anharmonicity that can include strong hydrogenbonding, tunneling, and vibrational resonances that dominate spectra, advanced theory is often required for even a qualitatively correct interpretation of spectra.

A suite of methods now exists for providing such computational insight. Anharmonic simulation methods range from targeted, variational simulations (or similar) on all or a select subset of vibrational modes¹⁹⁻²⁴ to more general approaches that do not require a priori selection of important vibrational motions

for larger systems. The latter are generally analogues of quantum chemistry methods for electronic structure, including vibrational self-consistent field (VSCF) theory²⁵⁻³⁵ and its correlated corrections: perturbation theories (VMP2³⁵ and VDPT2³⁶), configuration interaction (VCI), 27,37-41 and coupled-cluster theory (VCC). 37,42-Direct correlations from a harmonic reference are also possible. 45-47

In the VSCF method, for example, anharmonic motions are represented as one-dimensional "modals," which are the vibrational analogues of molecular orbitals:

$$\left[-\frac{1}{2} \frac{\partial^2}{\partial q_i^2} + \overline{V}_i^{\nu}(q_i) \right] \psi_i^{\nu}(q_i) = \varepsilon_i^{\nu} \psi_i^{\nu}(q_i) \tag{1}$$

(where vibration-rotation terms have been neglected and rectilinear coordinates have been assumed in the kinetic-energy operator, although neither of these attributes is required for VSCF). Each modal $\psi(q)$ for state ν vibrates in the mean field \overline{V} of the

a) Author to whom correspondence should be addressed: ryan.steele@utah.edu

remaining $3N_{atom}$ –7 modals, which can be obtained by integrating over the coupling to these other motions:

$$\overline{V}_{i}^{\nu}(q_{i}) = \left(\prod_{j \neq i}^{3N-7} \psi_{j}^{\nu}(q_{j}) | V(q_{1}, \dots, q_{3N-6}) | \prod_{j \neq i}^{3N-7} \psi_{j}^{\nu}(q_{j}) \right)$$
(2)

Because the effective potential depends on the remaining modals, the VSCF equations must be solved iteratively.

All of the aforementioned approaches share a common requirement, which is the need for a potential energy surface. Whether generated on-the-fly from quantum chemistry methods or via modern fitting techniques, $^{48-58}$ the practical reality remains that only small regions of these surfaces can typically be included in anharmonic vibrational calculations for all but the smallest chemical systems, due to the exponential scaling of multidimensional representations of these surfaces. One commonly used and effective route to selecting these regions is the so-called n-Mode Representation (n-MR), 26,28,59 which is effectively a many-body expansion of the ($3N_{atom}$ $^{-6}$)-dimensional potential energy surface (PES) with vibrational modes (in any coordinate system) as the component "bodies":

$$V^{n-MR}(q_1, q_2, \dots, q_{3N-6}) = V_0 + \sum_i \Delta V^{(1)}(q_i)$$

$$+ \sum_i \sum_{j>i} \Delta V^{(2)}(q_i, q_j)$$

$$+ \sum_i \sum_{j>i} \sum_{k>j} \Delta V^{(3)}(q_i, q_j, q_k) + \cdots$$
(3)

In this formulation, one-dimensional cuts through the PES comprise the first-order terms, $V^{(1)}(q_i) = V_0 + \sum_i \Delta V^{(1)}(q_i)$. Although this representation may form the canonical image of anharmonicity for many chemists (such as a Morse potential instead of a harmonic oscillator), it is decidedly insufficient for numerical simulations. For many vibrations, at least in rectilinear coordinate systems, a 1-MR potential often produces the wrong sign of the anharmonicity. Therefore, two-mode $\Delta V^{(2)}$ and higher couplings are required for accurate representations of most spectra. In practice, the *n*-MR expansion is truncated at some low order (often $\Delta V^{(2)}$ for molecules and complexes of substantive size 32,33,35,60-65) under the premise that this expansion should converge rapidly. The need to represent this pairwise (and possibly higher) coupling on semi-local quadrature grids serves as the overwhelming computational bottleneck for ab initio simulations of anharmonic spectroscopy. Even for the small water trimer case examined later in this work, for example, an 11-point Gauss-Hermite quadrature would require 2.5×10^4 , 1.8 \times 10⁶, and 8.8 \times 10⁷ potential energy evaluations for 2-, 3-, and 4-MR potentials, respectively. These values represent upper bounds to the requisite cost of such computations, as recent progress has been made in the area of sparse and adaptive grids. 66less, system-size scaling considerations necessarily limit many VSCF calculations to low-order truncations of the n-MR for even modestly sized systems. Although the limitation to pairwise couplings appears to be a rather drastic approximation to the full *n*-MR vibrational potential, errors on the order of ~10-20 cm⁻¹ are commonly observed.32 ^{0,62,64,71} making 2-MR calculations worth pursuing.

Practical experience with VSCF and truncated n-MR potentials suggests that performing these calculations can be a surprisingly fickle exercise. Particularly for larger molecules and systems with an appreciable density of low-frequency motions, the non-linear, iterative VSCF optimization often does not converge. Although some of this behavior can be rectified with improved SCF convergence techniques,⁷² other cases have routinely been found to be persistently non-convergent. Several examples will be assessed in this work (computational details described in Sec. III), but a preliminary description of their behavior highlights these outcomes. For example, although the water dimer yields a converged ground state, only 7 of the 12 excited fundamental VSCF states were found to converge; one of these nominally converged states exhibited an energy of approximately -449 000 cm⁻¹. Similar behavior was observed for the water trimer, wherein the ground state did not converge, only 6 of the 21 excited fundamentals converged, and three of the six convergent states yielded unphysical, negative transition

In this Article, this outcome is shown to often arise due to the existence of negative regions of the PES in truncated n-MR potentials. In other words, at truncated n, the PES can actually exhibit regions with potential energies below the global minimum. This paradoxical outcome can lead to deleterious consequences for VSCF calculations since, under certain conditions, dissociative effective potentials are obtained rather than bound vibrational systems. Therefore, in this brief analysis, we demonstrate how and why such behavior can be encountered with n-MR potentials and provide evidence that it is the source of VSCF convergence failures in certain cases, along with at least one simple solution to rectify this behavior. Of course, representing the potential at a higher order *n* could always rectify many of these issues, and several developments in recent years have extended the system-size range for which such an approach is feasible. 37,46,60,66-69,73-77 The present analysis remains useful for two reasons. First, sparse grids and prescreening techniques can provide access to 3- and 4-MR potentials for larger systems than naïve quadratures, but they must necessarily reach system-size limits, as well. The dearth of 4-MR-based spectroscopic analysis of polypeptides, for example, demonstrates that considerable work remains to make high-MR expansions a reality for systems of present interest. Second, an understanding of the origin of these negative potential regions provides an unexpected route to include only the most important, targeted 3-MR (or higher) couplings at dramatically reduced computational cost. This method is also symbiotic with, rather than orthogonal to, sparse-grid and pre-screening techniques, and a suitable combination of these techniques is encouraged.

Although no systematic analysis of this issue, to the present authors' knowledge, has appeared in the literature, some passing references to its existence have occurred.^{18,78} The accuracy of the *n*-MR approximation has been assessed in several instances (Refs. 40, 60, 71, 73, 74, and 79–83 among many others) but this *intrinsic pathology* has not. Furthermore, some understanding of this problem has likely existed, given some of the pragmatic approaches to achieving VSCF convergence in established codes (such as empirically scaling down the magnitude of mode couplings⁸⁴). For clarity, the pathologies encountered in the present potentials have nothing to do with "holes" from poorly sampled/fit analytic potentials nor with dissociative tails of Taylor-expansion representations of

potentials. Furthermore, this analysis focuses on single structures that are separated from other isomers/conformers by sufficiently high barriers that the ground-state vibrational wavefunctions do not traverse multiple minima, although this restriction is not required for the broader effect examined. The present analysis provides a more thorough description of the source of these pitfalls, along with at least one efficient and practical route to correct these issues.

II. THEORY AND ANALYSIS

Before presenting negative-potential results and corrections for general molecular systems, simple examples are warranted. For this purpose, the general conditions for negative potential regions to exist are first shown using a two-mode representation of a three-mode system. Subsequently, these negative regions are demonstrated to manifest as problematic regions for VSCF calculations under certain conditions of strong coupling. Finally, these concepts are shown to lead to problematic outcomes for low-order *n*-MR representations of real molecular potentials.

A. Existence of negative regions in truncated n-MR potentials

For a three-vibrational-mode system, such as a triatomic molecule or an equally sized subspace of a larger molecule, the 2-MR potential can be expressed as

$$V^{(2)}(q_1, q_2, q_3) = \left[V^{(1)}(q_1) + V^{(1)}(q_2) + V^{(1)}(q_3) \right]_{1-MR}$$

$$+ \left[\Delta V^{(2)}(q_1, q_2) + \Delta V^{(2)}(q_1, q_3) \right]_{2-MR}$$

$$+ \Delta V^{(2)}(q_2, q_3) \Big]_{2-MR}$$
(4)

where the 1- and 2-MR pieces are grouped separately. The fundamental concept underlying the existence of negative potentials is that a 2-MR potential is *not* merely a sum of two-displaced-mode potentials. Instead, it is a many-body potential that properly accounts for double-counting of pairs and their couplings. The first two 1-MR terms and the first 2-MR coupling term—i.e., $V^{(1)}(q_1) + V^{(1)}(q_2) + \Delta V^{(2)}(q_1,q_2) = V^{(2)}(q_1,q_2)$ —collectively comprise an example of a simple two-mode cut through the three-dimensional PES and a convenient reference point for this analysis. Because this cut involves displacements away from equilibrium (here taken to be the global minimum), this function is, by construction, positive-semidefinite and typically yields bound vibrational potentials if the original potential was also bound. Regrouping to isolate this term, the three-dimensional 2-MR potential becomes

$$V^{(2)}(q_1, q_2, q_3) = V^{(2)}(q_1, q_2) + \left[V^{(1)}(q_3) + \Delta V^{(2)}(q_1, q_3) + \Delta V^{(2)}(q_2, q_3)\right]$$
(5)

When mode q_3 is also displaced, the total function $V^{(2)}(q_1,q_2,q_3)$ can exhibit negative regions under certain conditions. The remaining terms in the expression explain this phenomenon: if the relaxation from the 1–3 and 2–3 mode pairs $[\Delta V^{(2)}(q_1,q_3) + \Delta V^{(2)}(q_2,q_3)]$ is sufficiently more negative than the 1D displace-

ment $V^{(1)}(q_3)$ [and the two-dimensional potential $V^{(2)}(q_1,q_2)$] is positive, then an overall negative potential can result. Qualitatively, these negative couplings correspond to substantive relaxation of a mode upon displacement by another mode, and sufficiently strong relaxations can induce the negative regions that are the focus of this work.

B. Persistence of negative regions in VSCF simulations

In the preceding example, displacement of *three* modes was required in order to observe negative regions of a 2-MR potential. Given that a general *n*-MR potential only requires *n*-dimensional quadratures, the role of these negative regions is not necessarily obvious for VSCF (and similar) calculations. In practical terms: why, for example, would negative regions upon three-mode displacement matter in a two-mode representation? As the following example demonstrates, such regions can nonetheless impact VSCF calculations.

For the same three-mode system and 2-MR potential, the effective, mean-field potential \overline{V} for mode 1 in a VSCF calculation would involve surviving terms of the following form,

$$\overline{V}_{1}^{\nu}(q_{1}) = V^{(1)}(q_{1}) + \langle \psi_{i}^{\nu} | \Delta V^{(2)}(q_{1}, q_{2}) | \psi_{i}^{\nu} \rangle_{q_{2}}
+ \langle \psi_{i}^{\nu} | \Delta V^{(2)}(q_{1}, q_{3}) | \psi_{i}^{\nu} \rangle_{q_{3}}
+ \langle V^{(1)}(q_{2}) \rangle_{q_{2}} + \langle V^{(1)}(q_{3}) \rangle_{q_{3}}
+ \langle \psi_{i}^{\nu} \psi_{i}^{\nu} | \Delta V^{(2)}(q_{2}, q_{3}) | \psi_{i}^{\nu} \psi_{i}^{\nu} \rangle_{q_{2}, q_{3}}$$
(6)

where the trailing subscripts denote the integration coordinate and ψ_i^{ν} represent states in the corresponding modals for coordinates q_2 and q_3 . The last three terms simply yield constant offsets for the q_1 potential. Because the coupling potentials $\Delta V^{(2)}$ —and not entire, intact, two-mode surfaces $V^{(2)}$ —are integrated, these integrals can sometimes yield strongly negative values. (The existence of negative values for these integrals alone is not intrinsically problematic and is, of course, required for anharmonic red-shifts. But when they are sufficient to overcome the bound nature of the 1D potentials, problems ensue. Strongly oscillatory terms in many-body expansions are well-known; 86-92 for vibrational problems, they take on special significance because they can qualitatively change the nature of the problem at truncated orders.) This 2-MR potential for mode 1 still involves displacement of this first mode and displacements of modes q_2 and q_3 . Therefore, displacement of three modes, albeit in pairwise increments, still enters VSCF calculations based on 2-MR potentials. Of course, in order for these terms to yield an unbound effective potential, the mode-coupling terms $\Delta V^{(2)}$ must be negative—at least in some regions of space where the modal wavefunctions are appreciable—and of sufficient magnitude to counteract the positive potential contained in $V^{(1)}(q_1)$. A practitioner of VSCF computations has no a priori means of predicting these magnitudes when computing the potentials, thereby leading to the somewhat unpredictable convergence behavior of VSCF for general molecular systems. The generality of this behavior should also be emphasized up front: This issue is neither limited to 2-MR potentials (although they are the focus here) nor rectilinear coordinate systems. Provided that the coupling is sufficiently strong, this

issue could ostensibly arise for any coordinate system and at any order of the n -MR.

C. Example of negative potentials

The behavior described above has been observed to occur in nearly all molecular systems of sufficient size, in our research group's experience. To tangibly demonstrate this effect, the PES for the protonated tropine molecule, C₈H₁₆NO⁺, using the B97-3⁹³/cc-pVDZ⁹⁴ (SG-3 quadrature grid⁹⁵) quantum chemistry method, is examined here. This molecule (hereafter termed tropineH⁺) would typically be considered "rigid" in general terms, but it nonetheless contains a hindered rotor that engenders large couplings when analyzed with rectilinear coordinate systems. It also contains an intramolecular hydrogen bond, involving the protonated amine (donor) and alcohol (acceptor), that leads to notable anharmonic shifts. Three normalmode displacements, shown at the top of Fig. 1 and involving the alcohol group's stretch and wag motions, form the focus of the present analysis. (The wag of the OH group is nearly identical in the latter two modes, but it forms in- and out-of-phase combinations with the tropine bridged bicyclic ring bending motions.) The three two-dimensional PESs for this triple of modes exhibit strong mode-pair couplings that are depicted in the lower portion of the

The two wag motions nearly cancel when displaced in opposite directions, leading to a flat potential in the anharmonic, two-dimensional scan of these motions. This behavior deviates notably from the harmonic potential but would still be adequately captured by the 2-MR potential. The OH stretch mode is particularly coupled to these wag motions, however. Displacement of the stretch in the compressed direction (positive displacement in Fig. 1) quickly reaches a steep, repulsive portion of the potential; displacement of each wag motion in either direction—because these rectilinear wags lead to elongation of the OH bond—leads to notable relaxation. This behavior yields strongly anharmonic and highly coupled motion of these three vibrations.

If, on the other hand, all three motions are simultaneously displaced, the 2-MR potential energy surface exhibits regions with potential energies below the equilibrium value. This behavior is depicted in Fig. 2, wherein OH wag A is maximally displaced along its quadrature grid and the remaining two vibrations' potential is plotted over the entirety of their pairwise grid. Any positive displacements of the OH stretch were found to generate negative potential-energy values when using the true global minimum as the zero of energy. Structures of representative points along this displaced surface (lettered for clarity) are shown in the lower panel of Fig. 2. The original wag A motion (in rectilinear displacements) leads to distortion of the O-H bond, and further displacement of wag B toward points a/d elongates this O-H coordinate in approximately the same direction; compression of wag B towards points c/e largely counteracts this motion (hence the steep repulsive potential in the real 3D potential). The relaxation engendered by displacement along the O-H stretch is sufficiently overestimated that the 2-MR potential dips steeply negative at both of these corners of the quadrature grid (points d and e). This effect stems from a rather simple source: In a 2-MR potential, the wag-stretch coupling is "doubly" relaxing, as the negative coupling appears in both wagstretch potentials. In the actual 3D potential, three-mode coupling

terms sufficiently counteract this relaxation and accurately reflect the response of the O–H bond.

The presence of these negative-potential regions is not merely a curious artifact of the n-MR. It instead leads to catastrophic problems in VSCF calculations, as discussed in Sec. II B. For the wag B normal mode of the same tropineH+ case, for example, these artifacts lead to inverted, unbound effective potentials in mean-field calculations of the v = 1 state with 2-MR, as shown in Fig. 3. Although early SCF cycles exhibit bound potentials for this case, the concavity of the effective, one-dimensional potential fully flips at iteration 14 and remains unbound thereafter. (The results shown in Fig. 3 were obtained with the Roothaan repeateddiagonalization method, which yields oscillatory solutions after cycle 25, but the same inverted-potential outcome was also obtained with the vDIIS algorithm.⁷²). The SCF procedure does not converge, and the SCF energy after 500 cycles is an unphysical -1.7 × 10⁶ cm⁻¹, which is consistent with the presence of both negative and unbound potentials. Similar behavior has been observed across a variety of molecules and vibrational motions in our research

To confirm that the modes involved in the negative pseudotriples were indeed responsible for this effect, the modes in the most-negative triple of tropineH+ were examined. As shown in Table S3 of the supplementary material and as will be discussed in more detail in Sec. III C, the (wag A)-(wag B)-(OH stretch) triple dominates the negative behavior, and this triple is the same set of modes depicted in Figs. 1 and 2. Accordingly, the contributions of the 2-MR (wag B)-(OH stretch) and (wag B)-(wag A) coupling terms to the wag B effective potential were computed separately; results are depicted in Fig. S1 of the supplementary material. These two terms alone contribute nearly the entirety of the negative-potential behavior. Because these terms contribute dissociative functions to the effective potential [as shown in the first sum of Eq. (6)] and because these terms are substantially more negative than the $V^{(1)}(q_{wagB})$ function is positive, these two couplings were confirmed to control this negative-effective-potential behavior. The coupling to the OH stretch is the strongest contributor, but both coupling terms contribute to the dissociative behavior.

III. CORRECTIONS AND IMPROVED METHODS

Given that the poor convergence behavior and unphysical energies were discovered to originate from negative potentials in truncated *n*-MR methods, the perhaps-obvious solution is to "paint in" higher-order couplings involving only these mode combinations. For example, if a 2-MR potential exhibits regions of negative mode triples, then these particular triples could be included to yield a pseudo-3-MR, hereafter denoted as a 2⁺³-MR. For clarity in philosophy, this correction was originally devised merely as a means to assess whether these problematic triples were, indeed, the source of the observed problems. Although it was (and still is) not intended as a replacement for more sophisticated means of accessing higher-order *n*-MR potentials, this approach was fortuitously discovered to be a particularly efficient correction scheme that is complementary to these existing methods. In the most straightforward of corrections, all triples with any quadrature point exhibiting a negative 2-MR value are included. Further refinements to this approach could include the triples with the most-negative

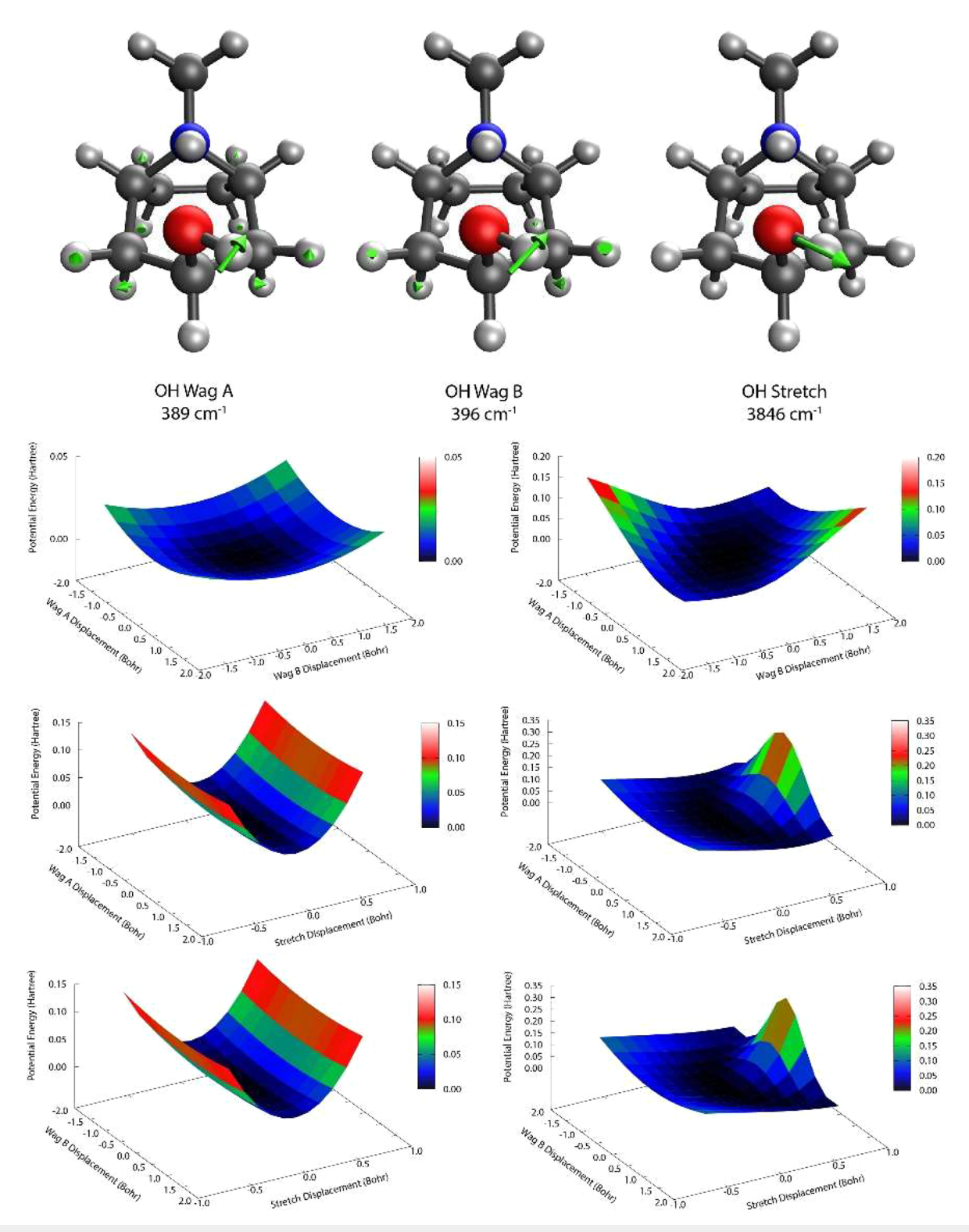


FIG. 1. Representative vibrational modes and potentials for tropineH⁺. (Upper panel) Normal-mode displacements, depicted as green arrows, in the equilibrium configuration. (Lower panels) Left column: Harmonic representation of each mode pair's two-dimensional potential energy surface. Right column: Actual, anharmonic potential energy surfaces. All calculations were performed with the B97-3/cc-pVDZ quantum chemistry method.

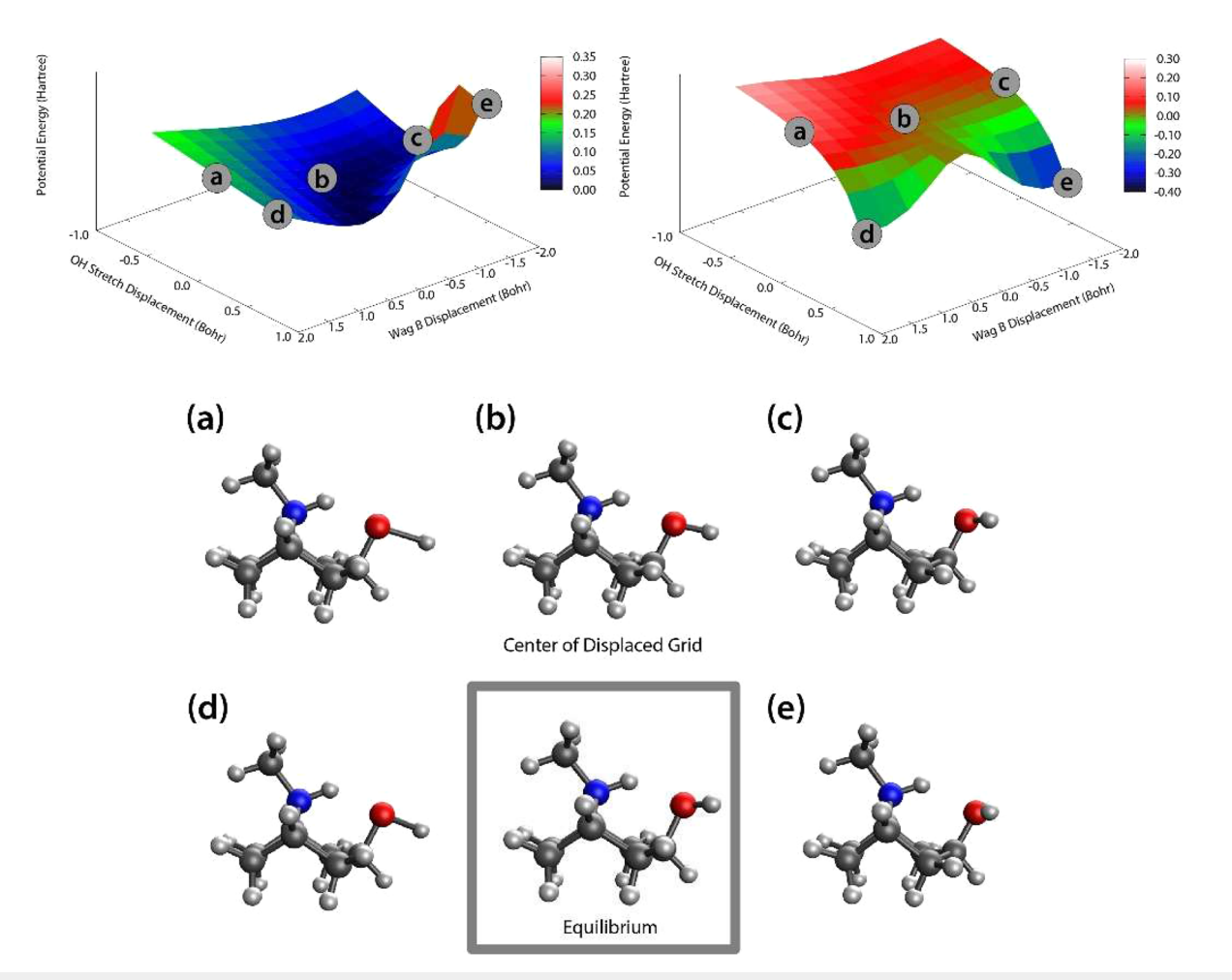


FIG. 2. Two-dimensional potential energy surfaces of the OH Stretch and Wag B normal modes of tropineH⁺, obtained at maximum displacement of the Wag A mode. Depicted are the actual 2D potential energy surface "cut" from a 3D scan (upper left panel), the 2-MR representation of the same cut (upper right panel), and structures [lower panel, (a)–(e)] corresponding to labeled points on the potential energy surfaces. All calculations were performed with the B97-3/cc-pVDZ quantum chemistry method, and the zero of energy is the global minimum.

regions, defined as (a) having the largest number of negative points, (b) the points with the most-negative values, (c) an integrated value of the coupling with the largest negative value, or some combination of these metrics. An analysis of some of these alternative strategies is included in the supplementary material and will be discussed in the context of the more straightforward 2^{+3} -MR results below.

In order to assess the behavior of this modified approach to the n-MR expansion, three test systems were examined. Small water clusters, including the dimer, $(H_2O)_2$ (12 vibrations), and trimer, $(H_2O)_3$ (21 vibrations), were first investigated using the MB-pol potential. These small test cases, combined with an analytic potential, provided the opportunity to examine both the 2^{+3} -MR approach and higher-order behavior up to 4-MR. The previously discussed protonated-tropine ion (72 vibrations) was also examined as a relatively large test system, using the same B97-3/cc-pVDZ *ab initio* potential as was presented in earlier fig-

ures. For this larger case, even the 3-MR was cost-prohibitive within this crude grid-based quadrature, and only the role of the targeted three-mode coupling correction was assessed. Quantum chemistry calculations were performed with the Q-Chem¹⁰⁵ software package.

Vibrational coordinates for the water clusters were window-localized (500-cm^{-1} window) modes, 106,107 and normal-mode coordinates were employed for protonated tropine. The VSCF calculations were performed in a basis set of ten harmonic oscillator functions with widths matched to the harmonic frequencies of each mode. Quadrature for the VSCF calculations was performed with a Gauss-Hermite grid of 11 points in each vibrational dimension and widths matched to the harmonic basis functions. The self-consistent field calculations were performed with the recently developed vDIIS algorithm⁷² and converged to a tolerance of 10^{-8} E_h in the maximum value of the DIIS error vector in all modes.

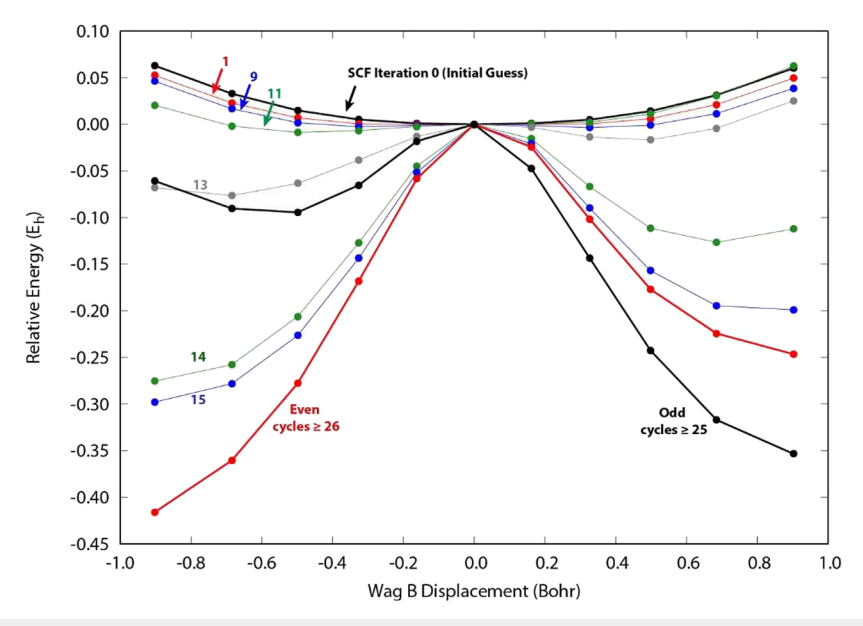


FIG. 3. One-dimensional VSCF effective potential energy curves of the Wag B normal mode of tropineH⁺. Representative SCF cycles are depicted, starting from an initial guess of 1D (uncoupled) modes. All potential-energy calculations were performed with the B97-3/cc-pVDZ quantum chemistry method.

A. Water dimer

A scan of the pseudo-3-MR potential—unique triples of mode displacements constructed from the 2-MR potential—for the water dimer yielded 16 triples (out of 220 total) that contained negative quadrature points. For this reason, the 2-MR-based VSCF calculation did not converge for five of the 12 fundamental transitions, and one of these nominally converged solutions exhibited an unphysical transition energy of -4.5×10^5 cm⁻¹. These results are shown in the 2-MR column of Table I. (All tabulated results are presented, without mode labels, according to the harmonic state ordering.).

Inclusion of the 16 triples in the 2⁺³-MR potential restored convergence to all computed states. Encouragingly, this approach also yielded transition energies that were surprisingly close to the 3- and 4-MR values. As a representative example, the two OH stretches that converged at all potential levels exhibited a frequency of 3610.7 cm⁻¹ with a standard 2-MR potential. (The degeneracy of these modes is a known artifact of local modes' neglect of bilinear couplings in meanfield methods. 81,106,107 Correlated-mode methods easily restore the splitting in these cases, 71,79,80 and the outcomes of the present analysis are unalerted by this behavior.) The 16 added triples restore 12.8 cm⁻¹ of the 15.7-cm⁻¹ difference between 2- and 3-MR results, indicating that these negative triples also account for much the strong coupling in this test system. This outcome is obtained despite the fact that the 2^{+3} -MR approach requires, in this rather small case, exactly one-tenth of the number of potential-energy evaluations of a full 3-MR potential.

Whether this numerical accuracy holds for correlated-mode calculations, such as VCI and similar, remains an open question and is worthy of future investigation. The fact that the reference VSCF states can be obtained at all (prior to subsequent correlation calculations) suggests that the original task of this method has

been accomplished; the reasonable numerical accuracy of the resulting states is a fortuitous, although explicable, outcome. Although the accuracy of correlated-mode calculations is likely more sensitive to these selections of terms, the method does appear to select the strongly coupled triples that would also, in turn, drive the most dominant mode-correlation corrections.

As shown in Sec. S1.A of the supplementary material, only (at most) 3 of these 16 added triples are required to converge the ground state and all fundamental transitions. Sequential addition of triples, ordered by either the number of negative quadrature points

TABLE I. Local-mode VSCF state energies (cm⁻¹) and transitions for the water dimer, using the MB-pol potential.

	2-MR		3-MR	4-MR
State	Standard	16 added triples	Standard	Standard
ZPE	10 408.6	10 487.3	10 490.5	10 486.8
1	a	286.0	299.4	291.7
2	368.9	424.7	431.6	428.8
3	368.9	424.7	431.6	428.8
4		161.3	162.9	161.7
5	-448737.9	441.1	441.0	432.8
6		611.3	614.6	608.3
7	1552.6	1583.2	1591.9	1589.9
8	1591.2	1640.0	1633.8	1630.5
9		3515.0	3513.5	3512.9
10	3610.7	3623.5	3626.4	3625.5
11	• • •	3630.6	3631.5	3630.0
12	3610.7	3623.5	3626.4	3625.5

^aOmitted states' VSCF procedure did not converge.

or by the integrated value of the negative portions of the potential, yielded nearly identical results. Perhaps intuitively, Mode 5, a water rocking mode and the state that exhibited a negative energy with the 2-MR potential, appears in four of the 16 negative triples, as well as the two strongest-negative triples by either metric. Therefore, a clear correlation between strength of negative coupling and spurious effective-potential behavior was observed. However, no clear gap in this ordered data was evident upon SCF convergence, suggesting that a well-defined cutoff in either metric is not yet predictive of convergence. Nonetheless, if a user wished to construct a minimal set of triples, ordering them by either metric appears to be a rational, albeit currently *ad hoc*, approach to determining this set.

B. Water trimer

For this slightly larger test system, 28 of the 1330 total triples exhibited negative values when constructed from the 2-MR potential. Accordingly, the ground state and 15 of the 21 fundamental transitions did not converge with VSCF; half of the converged states exhibited spuriously negative energies (Table II).

As was observed for the dimer, the 2⁺³-MR method restores convergence in all computed states of the trimer. The addition of these 28 selected triples yielded fundamental transitions that are within 2.7 cm⁻¹ (mean absolute deviation) of the full 3-MR

results. In fact, these 2⁺³-MR results are actually closer to 3-MR values than 3-MR is to 4-MR (3.7 cm⁻¹ MAD), indicating that this corrected 2-MR could perhaps be used as an efficient route to obtain adequate approximations of 3-MR spectra. This method exhibits a computational cost—defined here as the number of quadrature points required—that is 1.47 times higher than a standard 2-MR for this system but is also 28.2 times faster than a standard 3-MR.

Possible additional truncation of the included triples was once again examined in Sec. S1.B of the supplementary material. In this case, the ordering of the included triples (by number of negative points or by negative integral value) was again qualitatively similar between the two approaches. The ground vibrational state required 2-3 added triples to converge, and 15-16 added triples were required to converge all of the fundamentals' states. Therefore, only roughly half of the negative triples are needed in order to yield convergence, which suggests that at least some of the negative regions are either sufficiently small in magnitude or fall outside of the region of basis-function significance to influence convergence. At present, given the need to perform successive SCF calculations until convergence is reached in these alternative methods, the 2+3-MR method is recommended as a well-defined improvement over 2-MR. Future investigation into more predictive truncations of these negative triples is nonetheless encouraged.

TABLE II. Local-mode VSCF state energies (cm⁻¹) and transitions for the water trimer, using the MB-pol potential.

State	2-MR		3-MR	4-MR
	Standard	26 added triples	Standard	Standard
ZPE	(16 341.9) ^a	16 493.0	16 479.3	16 472.4
1	b	381.1	382.5	378.2
2		383.9	383.8	379.5
3		201.2	200.0	198.4
4		206.0	204.7	203.0
5		207.4	204.9	203.2
6		444.2	444.0	439.7
7	-563 476.3	516.2	510.2	501.6
8	$-566\ 080.8$	503.7	495.6	487.3
9	-563 461.8	508.2	501.6	493.4
10		670.8	667.4	661.6
11		707.0	703.3	696.8
12		695.1	692.7	686.4
13		1633.4	1627.9	1624.4
14		1634.8	1628.9	1625.5
15		1635.7	1629.8	1626.4
16	3 416.8	3427.5	3427.8	3428.1
17	3 414.3	3424.7	3425.1	3425.4
18	3 426.4	3440.4	3440.3	3440.5
19		3621.4	3620.3	3618.9
20		3626.1	3625.1	3623.6
21		3625.6	3625.1	3623.8

^aGround state did not converge; last iteration's energy retained for computing transition energies.

^bOmitted states' VSCF procedure did not converge.

C. Protonated tropine

Finally, the tropineH⁺ ion that was the focus of Sec. II is revisited here. This case represents an approximate lower system-size bound to the type of biologically and/or pharmacologically relevant molecules that could ostensibly be investigated by anharmonic simulation methods, provided that both computational cost considerations and the present qualitative deficiencies can be addressed. This ion exhibits 72 vibrational modes and would be considered a routine harmonic calculation for all but the most demanding quantum chemistry methods. However, a full 3-MR quadrature

(without sparse-grid techniques) would require 7.94×10^7 potential-energy evaluations with the present 11-point Gauss-Hermite grid, either making anharmonic, *ab initio* spectroscopy simulations cost-prohibitive or necessitating spectroscopically inaccurate potentials.

An analysis of 2-MR-based triples of modes indicated that only 19 of the 59 640 total triples exhibited negative regions for tropineH⁺. These 19 triples were sufficient to render 33 of the 72 fundamentals non-convergent, and one of the remnant fundamentals converged to a large, negative value (Table III). Inclusion of

TABLE III. Normal-mode VSCF state energies (cm⁻¹) and transitions for the protonated tropine ion, using the B97-3/cc-pVDZ method.

	2-MR			2-MR	
State	Standard	Add 19 triples	State (cont.)	Standard	Add 19 triples
ZPE	53 210.9	53 244.7			
1	a	138.5	37		1244.9
2		224.1	38		1269.1
3	310.7	319.4	39	1286.4	1286.3
4		264.4	40	1304.0	1304.9
5	303.2	303.4	41	1318.0	1318.1
6	350.9	358.5	42		1343.4
7	354.3	354.6	43	• • •	1338.1
8	430.2	502.2	44		1352.4
9	$-371\ 522.8$	533.7	45	1364.3	1364.0
10	460.0	472.4	46		1372.0
11		523.1	47		1402.0
12		531.7	48		1416.9
13	696.5	696.6	49		1435.7
14	704.1	704.2	50	1444.2	1443.6
15		758.2	51		1463.1
16	790.9	790.5	52	1463.1	1462.8
17	812.9	813.0	53	1461.9	1461.3
18	857.4	857.4	54	1477.4	1477.6
19	862.6	862.3	55	1503.1	1502.7
20	892.5	891.9	56		1500.3
21	930.7	930.9	57		2953.5
22		945.7	58		2988.4
23	955.2	954.9	59		2967.9
24		1010.3	60	2973.4	2973.7
25	1 014.3	1014.2	61		3002.2
26	1 025.0	1024.5	62	3005.4	3005.5
27	1 031.4	1031.0	63		3000.2
28		1084.0	64	3006.6	3006.6
29		1105.7	65	3033.6	3033.6
30		1117.6	66	3030.8	3030.8
31		1163.9	67	3017.4	3017.5
32		1168.7	68	3050.0	3049.9
33		1196.4	69	2987.3	2985.0
34		1204.0	70		3040.8
35		1220.6	71	2994.4	2994.6
36	1 229.5	1229.4	72	3558.6	3579.3

^aOmitted states' VSCF procedure did not converge.

these 19 triples (at a total 2⁺³-MR cost that is only 0.4% of the cost of a full 3-MR quadrature!) restores convergence in all of these states. The analysis in Sec. S1.C of the supplementary material indicates that only a single triple—the same triple featured in Figs. 1 and 2—is actually necessary to restore convergence. Because of the high computational cost of the 3- and 4-MR potentials, no comparison to these reference results was performed for this test case. Nonetheless, the restoration of even qualitatively correct SCF behavior (at a 2⁺³-MR cost that is only 8% higher than the reference 2-MR) is the main outcome of this analysis and suggests that these negative-potential considerations should become a *de facto* component of VSCF calculations for all but the smallest molecular systems.

IV. SUMMARY

Computed vibrational spectra that include anharmonic corrections have become key connections between modern vibrational experiments and theoretical analysis. For all but small, rigid molecules, however, low-order truncations of the *n*-mode representation of the vibrational potential can often lead to poor convergence of vibrational self-consistent field calculations or even convergence to meaningless, negative energies. In this brief analysis, a dominant source of this behavior was traced to negative regions—literal pitfalls—in the truncated *n*-MR potential, which, in turn, generate unbound effective potentials for the vibrational modals.

An understanding of this problem's origin also provided a surprisingly simple (although not unique) method to correct it. The inclusion of three-mode couplings—only for the mode triples exhibiting negative regions—corrected the SCF convergence problems for all of the test cases considered here. Therefore, this correction is recommended for all 2-MR VSCF calculations when feasible. Future analyses may also generate even more efficient methods to select these targeted triples.

Because the negative regions stem from strong pairwise mode couplings, this new 2+3-MR method was empirically found to include most of the strong three-mode couplings. Thus, the same method used to qualitatively correct the unbound effective potentials was also found to closely—but not perfectly—approximate full 3-MR VSCF results at dramatically reduced cost (28× faster for the water trimer and 240× faster for protonated tropine). In cases of particularly strong coupling, the same method could be used as a 3⁺⁴-MR potential or even stacked in a 23+4-MR form when the corrected potential itself still yields sufficiently negative quadruples. Continued investigation of the triples necessary for the latter approach is still required, although we anecdotally note that we have encountered particularly "floppy," biologically relevant cases in other applications where the existence of negative pseudo-quadruples led to poor convergence.

Of course, the strongest anharmonic couplings often stem from vibrational mode representations or coordinate systems that are not optimally suited to the vibrational problem being investigated. For some of the embedded-rotor modes considered in this work, for example, curvilinear coordinate systems and quadratures could reduce or eliminate at least some of these issues. Rectilinear coordinate systems are a convenient choice for general, large

molecules and clusters, although generic curvilinear alternatives also exist. 108-113 The existence of negative potentials could perhaps be used as a means to assess the appropriateness of coordinate systems. This occurrence of negative potentials is not necessarily limited to rotors or other naturally curvilinear motions, however. In our experience, even polyenes (data not shown in this work), which would normally be considered "rigid" by anharmonic-spectroscopy standards, have required the addition of selected triples to a 2-MR in order to reach VSCF convergence. Moreover, cases of strongly coupled curvilinear motions—yielding nearly rectilinear displacements through strong coupling—would be subject to the same pathologies described herein, and the same approaches to identify and correct these cases would be appropriate. Taylor expansions of vibrational potentials are ostensibly subject to the same issues, although such methods often trade some accuracy within single-mode potentials for higher-order couplings. A full quartic potential, for example, is unlikely to encounter these negative regions (while possibly generating others⁸⁵), although truncated *n*-MR quartic potentials¹¹⁴ could exhibit them.

Furthermore, local modes \$1,106,107,115,116\$ are sometimes more susceptible to this effect than their normal-mode counterparts. In hindsight, this outcome is intuitive: local modes are known to shift a series of possibly high-order, normal-mode couplings to low-order couplings at short distances. \$106,107,116\$ If the low orders of the \$n\$-MR are especially strong, then negative potentials are sometimes more likely to be encountered. Fortunately, the now-established distance decay of these couplings provides an especially efficient route to include them, and the addition of negative triples (as just one example) within a short cutoff distance would be a computationally efficient route to correct for these issues. Future analyses could examine the interplay between this distance dependence of couplings and negative potential regions.

Pathological behavior in low-order truncations of the *n*-MR expansion should, of course, be placed in the context of more general methods that allow for less aggressive truncations. As noted in the Introduction, sparse and/or adaptive grids, ^{66–70} sum-of-products potentials, 117 and pre-screening/recycling techniques 73,77,97-100 all serve to expand the scope of system sizes for which higher-order *n*-MR potentials are accessible. Such methods "delay the inevitable," in the sense that the scaling of both the n-MR terms and the underlying potential energy surface will eventually require more substantive truncations. Vibrational potentials in full dimensionality beyond 2-MR are, at present, exceedingly rare for biologically relevant molecules, for example. 32,60 Nonetheless, such methods are also potentially symbiotic with the present approach. Prescreening methods ostensibly serve a similar purpose, in that they use low-level estimates to determine significant mode couplings. The present method provides an essentially "free" means of determining the set of mode triples (or higher) that are necessary for VSCF convergence without pre-screening, although it also does not systematically estimate the strength of such couplings as would occur in pre-screening methods. The 2⁺³-MR method could, for example, be used to determine whether a pre-screened 3-MR is actually needed. Perhaps more importantly, it also provides a qualitative explanation of cases where even efficiently pre-screened *n*-MR

Overall, this analysis explains some of the most problematic (and, frankly, frustrating) aspects of VSCF calculations of large molecules and provides at least one route to correct such problems at little added computational cost. It also achieves VSCF convergence without rescaling⁸⁴ of mode-coupling potentials. Whether this straightforward correction is the ideal approach, or whether alternative formulations of the *n*-MR should instead be pursued, remains an open question for future investigation.

SUPPLEMENTARY MATERIAL

The supplementary material includes an analysis of the addition of three-mode couplings for the three test systems presented in the main text. Comparison of two metrics for ordering the strength of these couplings is provided.

ACKNOWLEDGMENTS

E.L.Y. and R.P.S. acknowledge funding from the Department of Energy under Grant No. DE-SC0019405 for the analysis and development of these negative potential methods. R.J.S. and R.P.S. acknowledge funding from the National Science Foundation under Grant No. CHE-2102309 for analysis of mode coupling in the water clusters. The support and resources from the Center for High-Performance Computing at The University of Utah are gratefully acknowledged. This work also used the Extreme Science and Engineering Discovery Environment (XSEDE), which is supported by the National Science Foundation Grant No. ACI-1548562.

AUTHOR DECLARATIONS

Conflict of Interest

The authors have no conflicts to disclose.

Author Contributions

Emily L. Yang: Conceptualization (equal); Data curation (equal); Formal analysis (equal); Investigation (equal); Methodology (equal); Software (lead); Validation (equal); Visualization (equal); Writing original draft (supporting); Writing - review & editing (supporting). Justin J. Talbot: Conceptualization (supporting); Formal analysis (supporting); Investigation (supporting); Methodology (supporting); Software (supporting); Writing - review & editing (supporting). Ryan J. Spencer: Conceptualization (supporting); Formal analysis (supporting); Investigation (supporting); Methodology (supporting); Software (supporting); Writing review & editing (supporting). Ryan P. Steele: Conceptualization (equal); Data curation (equal); Formal analysis (equal); Funding acquisition (lead); Investigation (equal); Methodology (equal); Project administration (lead); Resources (lead); Software (supporting); Supervision (lead); Validation (equal); Visualization (equal); Writing - original draft (lead); Writing - review & editing

DATA AVAILABILITY

The data that support the findings of this study are available within the article and its supplementary material.

REFERENCES

- ¹T. L. Guasco and M. A. Johnson, *Emerging Trends in Chemical Applications of Lasers* (American Chemical Society, 2021), Vol. 1398, pp. 277–306.
- ²H. J. Zeng and M. A. Johnson, "Demystifying the diffuse vibrational spectrum of aqueous protons through cold cluster spectroscopy," Annu. Rev. Phys. Chem. 72(1), 667–691 (2021).
- ³N. Yang, T. Khuu, S. Mitra, C. H. Duong, M. A. Johnson, R. J. DiRisio, A. B. McCoy, E. Miliordos, and S. S. Xantheas, "Isolating the contributions of specific network sites to the diffuse vibrational spectrum of interfacial water with isotopomer-selective spectroscopy of cold clusters," J. Phys. Chem. A 124(50), 10393–10406 (2020).
- ⁴N. C. Polfer, "Infrared multiple photon dissociation spectroscopy of trapped ions," Chem. Soc. Rev. **40**(5), 2211–2221 (2011).
- ⁵A. B. Wolk, C. M. Leavitt, E. Garand, and M. A. Johnson, "Cryogenic ion chemistry and spectroscopy," Acc. Chem. Res. 47(1), 202–210 (2014).
- ⁶E. Garand, "Spectroscopy of reactive complexes and solvated clusters: A bottomup approach using cryogenic ion traps," J. Phys. Chem. A **122**(32), 6479–6490 (2018)
- ⁷B. M. Marsh, J. M. Voss, and E. Garand, "A dual cryogenic ion trap spectrometer for the formation and characterization of solvated ionic clusters," J. Chem. Phys. **143**(20), 204201 (2015).
- ⁸C. M. Leavitt, A. B. Wolk, J. A. Fournier, M. Z. Kamrath, E. Garand, M. J. Van Stipdonk, and M. A. Johnson, "Isomer-specific IR–IR double resonance spectroscopy of D₂-tagged protonated dipeptides prepared in a cryogenic ion trap," J. Phys. Chem. Lett. **3**(9), 1099–1105 (2012).
- ⁹J. Martens, G. Berden, C. R. Gebhardt, and J. Oomens, "Infrared ion spectroscopy in a modified quadrupole ion trap mass spectrometer at the felix free electron laser laboratory," Rev. Sci. Instrum. 87(10), 103108 (2016).
- ¹⁰P. B. Armentrout, B. C. Stevenson, M. Ghiassee, G. C. Boles, G. Berden, and J. Oomens, "Infrared multiple-photon dissociation spectroscopy of cationized Glycine: Effects of alkali metal cation size on gas-phase conformation," Phys. Chem. Chem. Phys. 24(37), 22950–22959 (2022).
- ¹¹A. B. McCoy, T. L. Guasco, C. M. Leavitt, S. G. Olesen, and M. A. Johnson, "Vibrational manifestations of strong non-condon effects in the $H_3O^+\cdot X_3$ (X = Ar, N_2 , CH₄, H_2O) complexes: A possible explanation for the intensity in the 'association band' in the vibrational spectrum of water," Phys. Chem. Chem. Phys. 14(20), 7205–7214 (2012).
- ¹²J. J. Talbot, X. Cheng, J. D. Herr, and R. P. Steele, "Vibrational signatures of electronic properties in oxidized water: Unraveling the anomalous spectrum of the water dimer cation," J. Am. Chem. Soc. 138(36), 11936–11945 (2016).
- ¹³O. Vendrell, F. Gatti, and H.-D. Meyer, "Dynamics and infrared spectroscopy of the protonated water dimer," Angew. Chem., Int. Ed. 46(36), 6918–6921 (2007).
- ¹⁴C. H. Duong, N. Yang, M. A. Johnson, R. J. DiRisio, A. B. McCoy, Q. Yu, and J. M. Bowman, "Disentangling the complex vibrational mechanics of the protonated water trimer by rational control of its hydrogen bonds," J. Phys. Chem. A 123(37), 7965–7972 (2019).
- ¹⁵J. J. Talbot, N. Yang, M. Huang, C. H. Duong, A. B. McCoy, R. P. Steele, and M. A. Johnson, "Spectroscopic signatures of mode-dependent tunnel splitting in the iodide-water binary complex," J. Phys. Chem. A 124(15), 2991–3001 (2020).
- ¹⁶E. Castro-Juárez, X.-G. Wang, T. Carrington, Jr., E. Quintas-Sánchez, and R. Dawes, "Computational study of the Ro-vibrational spectrum of CO-CO₂," J. Chem. Phys. 151(8), 084307 (2019).
- ¹⁷M. Schröder, F. Gatti, D. Lauvergnat, H.-D. Meyer, and O. Vendrell, "The coupling of the hydrated proton to its first solvation shell," Nat. Commun. **13**(1), 6170 (2022).
- ¹⁸M. Schröder and H.-D. Meyer, "Calculation of the vibrational excited states of malonaldehyde and their tunneling splittings with the multi-configuration timedependent hartree method," J. Chem. Phys. 141(3), 034116 (2014).
- ¹⁹P. M. Felker and Z. Bačić, "Intermolecular vibrational states of HF trimer from rigorous nine-dimensional quantum calculations: Strong coupling between intermolecular bending and stretching vibrations and the importance of the three-body interactions," J. Chem. Phys. **157**(19), 194103 (2022).
- ²⁰T. Carrington, Jr., "Perspective: Computing (ro-)vibrational spectra of molecules with more than four atoms," J. Chem. Phys. **146**(12), 120902 (2017).

- ²¹ T. Carrington, Jr., "Using iterative methods to compute vibrational spectra," in *Handbook of High-Resolution Spectroscopy* (John Wiley & Sons, 2011).
- ²²T. Carrington, Jr. and X.-G. Wang, "Computing ro-vibrational spectra of van der Waals molecules," Wiley Interdiscip. Rev.: Comput. Mol. Sci. 1(6), 952–963 (2011).
- ²³ P. M. Felker and Z. Bačić, "Noncovalently bound molecular complexes beyond diatom-diatom systems: Full-dimensional, fully coupled quantum calculations of rovibrational states," Phys. Chem. Chem. Phys. **24**(40), 24655–24676 (2022).
- 24 B. Yang, P. Zhang, C. Qu, P. C. Stancil, J. M. Bowman, N. Balakrishnan, and R. C. Forrey, "Full-dimensional quantum dynamics of SO($X^3\Sigma^-$) in collision with H_2 ," Chem. Phys. **532**, 110695 (2020).
- ²⁵J. M. Bowman, "Self-consistent field energies and wavefunctions for coupled oscillators," J. Chem. Phys. 68(2), 608–610 (1978).
- ²⁶J. M. Bowman, "The self-consistent-field approach to polyatomic vibrations," Acc. Chem. Res. 19(7), 202–208 (1986).
- ²⁷S. Carter, J. M. Bowman, and N. C. Handy, "Extensions and tests of 'multimode': A code to obtain accurate vibration/rotation energies of many-mode molecules," Theor. Chem. Acc. 100(1-4), 191-198 (1998).
- ²⁸S. Carter, S. J. Culik, and J. M. Bowman, "Vibrational self-consistent field method for many-mode systems: A new approach and application to the vibrations of CO adsorbed on Cu(100)," J. Chem. Phys. **107**(24), 10458–10469 (1997).
- ²⁹K. M. Christoffel and J. M. Bowman, "Investigations of self-consistent field, SCF CI and virtual stateconfiguration interaction vibrational energies for a model three-mode system," Chem. Phys. Lett. **85**(2), 220–224 (1982).
- ³⁰ M. Keçeli and S. Hirata, "Size-extensive vibrational self-consistent field method," J. Chem. Phys. 135(13), 134108 (2011).
- ³¹ O. Christiansen, "A second quantization formulation of multimode dynamics," J. Chem. Phys. **120**(5), 2140–2148 (2004).
- ³²T. K. Roy, R. Sharma, and R. B. Gerber, "First-principles anharmonic quantum calculations for peptide spectroscopy: VSCF calculations and comparison with experiments," Phys. Chem. Chem. Phys. **18**(3), 1607–1614 (2016).
- ³³T. K. Roy and R. B. Gerber, "Vibrational self-consistent field calculations for spectroscopy of biological molecules: New algorithmic developments and applications," Phys. Chem. Chem. Phys. 15(24), 9468–9492 (2013).
- 34. S. Hirata, M. Keçeli, and K. Yagi, "First-principles theories for anharmonic lattice vibrations," J. Chem. Phys. 133(3), 034109 (2010).
- ³⁵R. B. Gerber, G. M. Chaban, B. Brauer, and Y. Miller, *Theory and Applications of Computational Chemistry: The First 40 Years* (Elsevier, Amsterdam, The Netherlands, 2005), pp. 165–193.
- ³⁶N. Matsunaga, G. M. Chaban, and R. B. Gerber, "Degenerate perturbation theory corrections for the vibrational self-consistent field approximation: Method and applications," J. Chem. Phys. 117(8), 3541–3547 (2002).
- ³⁷O. Christiansen, "Selected new developments in vibrational structure theory: Potential construction and vibrational wave function calculations," Phys. Chem. Chem. Phys. 14(19), 6672–6687 (2012).
- 38 T. Mathea, T. Petrenko, and G. Rauhut, "Advances in vibrational configuration interaction theory- Part 2: Fast screening of the correlation space," J. Comput. Chem. $43(1),6{-}18\ (2022).$
- ³⁹T. Mathea and G. Rauhut, "Advances in vibrational configuration interaction theory- part 1: Efficient calculation of vibrational angular momentum terms," J. Comput. Chem. 42(32), 2321–2333 (2021).
- ⁴⁰P. T. Panek, A. A. Hoeske, and C. R. Jacob, "On the choice of coordinates in anharmonic theoretical vibrational spectroscopy: Harmonic vs Anharmonic coupling in vibrational configuration interaction," J. Chem. Phys. 150(5), 054107 (2019).
- ⁴¹T. C. Thompson and D. G. Truhlar, "SCF CI calculations for vibrational eigenvalues and wavefunctions of systems exhibiting fermi resonance," Chem. Phys. Lett. 75(1), 87–90 (1980).
- ⁴²C. König and O. Christiansen, "Automatic determination of important mode-mode correlations in many-mode vibrational wave functions," J. Chem. Phys. 142(14), 144115 (2015).
- ⁴³I. H. Godtliebsen, B. Thomsen, and O. Christiansen, "Tensor decomposition and vibrational coupled cluster theory," J. Phys. Chem. A 117(32), 7267–7279 (2013).

- ⁴⁴O. Christiansen, "Vibrational coupled cluster theory," J. Chem. Phys. **120**(5), 2149–2159 (2004).
- ⁴⁵P. R. Franke, J. F. Stanton, and G. E. Douberly, "How to VPT2: Accurate and intuitive simulations of CH stretching infrared spectra using VPT2+K with large effective Hamiltonian resonance treatments," J. Phys. Chem. A **125**(6), 1301–1324 (2021).
- ⁴⁶R. Ramakrishnan and G. Rauhut, "Semi-quartic force fields retrieved from multi-mode expansions: Accuracy, scaling behavior, and approximations," J. Chem. Phys. 142(15), 154118 (2015).
- ⁴⁷C. Y. Lin, A. T. B. Gilbert, and P. M. W. Gill, "Calculating molecular vibrational spectra beyond the harmonic approximation," Theor. Chem. Acc. **120**(1–3), 23–35 (2008).
- ⁴⁸E. Lambros, S. Dasgupta, E. Palos, S. Swee, J. Hu, and F. Paesani, "General many-body framework for data-driven potentials with arbitrary quantum mechanical accuracy: Water as a case study," J. Chem. Theory Comput. 17(9), 5635–5650 (2021).
- ⁴⁹E. F. Bull-Vulpe, M. Riera, S. L. Bore, and F. Paesani, "Data-driven many-body potential energy functions for generic molecules: Linear alkanes as a proof-of-concept application," J. Chem. Theory Comput. **19**, 4494 (2022).
- ⁵⁰R. Conte, C. Qu, P. L. Houston, and J. M. Bowman, "Efficient generation of permutationally invariant potential energy surfaces for large molecules," J. Chem. Theory Comput. **16**(5), 3264–3272 (2020).
- ⁵¹ A. Nandi, C. Qu, P. L. Houston, R. Conte, Q. Yu, and J. M. Bowman, "A CCSD(T)-Based 4-body potential for water," J. Phys. Chem. Lett. **12**(42), 10318–10324 (2021).
- ⁵²E. Quintas-Sánchez and R. Dawes, "Spectroscopy and scattering studies using interpolated *ab initio* potentials," Annu. Rev. Phys. Chem. **72**(1), 399–421 (2021).
- ⁵³E. Quintas-Sánchez and R. Dawes, "Autosurf: A freely available program to construct potential energy surfaces," J. Chem. Inf. Model. **59**(1), 262–271 (2019).
- ⁵⁴Z. Xie and J. M. Bowman, "Permutationally invariant polynomial basis for molecular energy surface fitting via monomial symmetrization," J. Chem. Theory Comput. **6**(1), 26–34 (2010).
- ⁵⁵O. T. Unke, S. Chmiela, M. Gastegger, K. T. Schütt, H. E. Sauceda, and K.-R. Müller, "Spookynet: Learning force fields with electronic degrees of freedom and nonlocal effects," Nat. Commun. **12**(1), 7273 (2021).
- ⁵⁶P. Friederich, F. Häse, J. Proppe, and A. Aspuru-Guzik, "Machine-learned potentials for next-generation matter simulations," Nat. Mater. **20**(6), 750–761 (2021).
- ⁵⁷T. W. Ko, J. A. Finkler, S. Goedecker, and J. Behler, "A fourth-generation highdimensional neural network potential with accurate electrostatics including nonlocal charge transfer," Nat. Commun. **12**(1), 398 (2021).
- ⁵⁸J. Behler and M. Parrinello, "Generalized neural-network representation of high-dimensional potential-energy surfaces," Phys. Rev. Lett. **98**(14), 146401 (2007).
- ⁵⁹Q. Yu, C. Qu, P. L. Houston, R. Conte, A. Nandi, and J. M. Bowman, *Vibrational Dynamics of Molecules* (World Scientific, 2021), pp. 296–339.
- M. Bounouar and C. Scheurer, "Reducing the vibrational coupling network in N-methylacetamide as a model for *ab initio* infrared spectra computations of peptides," Chem. Phys. 323(1), 87–101 (2006).
 L. Pele and R. B. Gerber, "On the number of significant mode-mode anhar-
- ⁵¹L. Pele and R. B. Gerber, "On the number of significant mode-mode anharmonic couplings in vibrational calculations: Correlation-corrected vibrational self-consistent field treatment of di-, tri-, -and tetrapeptides," J. Chem. Phys. 128(16), 165105 (2008).
- ⁶²T. K. Roy, T. Carrington, Jr., and R. B. Gerber, "Approximate first-principles anharmonic calculations of polyatomic spectra using MP2 and B3LYP potentials: Comparisons with experiment," J. Phys. Chem. A 118(33), 6730–6739 (2014).
- ⁶³ A. Erba, J. Maul, M. Ferrabone, R. Dovesi, M. Rerat, and P. Carbonniere, "Anharmonic vibrational states of solids from DFT calculations. Part II: Implementation of the VSCF and VCI methods," J. Chem. Theory Comput. 15(6), 3766–3777 (2019).
- ⁶⁴T. K. Roy and R. B. Gerber, "Dual basis approach for *ab initio* anharmonic calculations of vibrational spectroscopy: Application to microsolvated biomolecules," J. Chem. Theory Comput. **16**(11), 7005–7016 (2020).
- 65 J. O. Jung and R. B. Gerber, "Vibrational wave functions and spectroscopy of $(H_2\mathrm{O})_n,\ n=2,\ 3,\ 4,\ 5:$ Vibrational self-consistent field with correlation corrections," J. Chem. Phys. $105(23),\ 10332-10348\ (1996).$

- ⁶⁶ J. Cooper and T. Carrington, Jr., "Computing vibrational energy levels by using mappings to fully exploit the structure of a pruned product basis," J. Chem. Phys. **130**(21), 214110 (2009).
- ⁶⁷S. Manzhos, K. Yamashita, and T. Carrington, "Fitting sparse multidimensional data with low-dimensional terms," Comput. Phys. Commun. **180**(10), 2002–2012 (2009).
- ⁶⁸S. Manzhos and T. Carrington, Jr., "A random-sampling high dimensional model representation neural network for building potential energy surfaces," J. Chem. Phys. 125(8), 084109 (2006).
- ⁶⁹M. Sparta, D. Toffoli, and O. Christiansen, "An adaptive density-guided approach for the generation of potential energy surfaces of polyatomic molecules," Theor. Chem. Acc. **123**(5-6), 413–429 (2009).
- ⁷⁰D. Strobusch and C. Scheurer, "Adaptive sparse grid expansions of the vibrational Hamiltonian," J. Chem. Phys. **140**(7), 074111 (2014).
- ⁷¹ P. T. Panek and C. R. Jacob, "On the benefits of localized modes in anharmonic vibrational calculations for small molecules," J. Chem. Phys. **144**(16), 164111 (2016).
- ⁷²E. L. Yang, R. J. Spencer, A. A. Zhanserkeev, J. J. Talbot, and R. P. Steele, "Accelerating and stabilizing the convergence of vibrational self-consistent field calculations via the Direct inversion of the iterative subspace (vDIIS) algorithm," J. Chem. Phys. 159(8), 084103 (2023).
- ⁷³M. Sparta, I.-M. Høyvik, D. Toffoli, and O. Christiansen, "Potential energy surfaces for vibrational structure calculations from a multiresolution adaptive density-guided approach: Implementation and test calculations," J. Phys. Chem. A 113(30), 8712–8723 (2009).
- ⁷⁴D. Madsen, O. Christiansen, and C. König, "Anharmonic vibrational spectra from double incremental potential energy and dipole surfaces," Phys. Chem. Chem. Phys. 20(5), 3445–3456 (2018).
- ⁷⁵G. Rauhut, "Efficient calculation of potential energy surfaces for the generation of vibrational wave functions," J. Chem. Phys. **121**(19), 9313–9322 (2004).
- ⁷⁶D. M. Benoit, "Fast vibrational self-consistent field calculations through a reduced mode-mode coupling scheme," J. Chem. Phys. 120(2), 562–573 (2003).
- 77 A. A. Zhanserkeev, E. L. Yang, and R. P. Steele, "Accelerating anharmonic spectroscopy simulations via local-mode, multilevel methods," J. Chem. Theory Comput. 19(16), 5572–5585 (2023).
- 78 L. M. Serafin, "Chemical bonding properties in substituted disilynes," Ph.D. thesis, University of St Andrews, 2012.
- ⁷⁹P. T. Panek and C. R. Jacob, "Efficient calculation of anharmonic vibrational spectra of large molecules with localized modes," ChemPhysChem **15**(15), 3365–3377 (2014).
- ⁸⁰ M. W. D. Hanson-Heine, "Examining the impact of harmonic correlation on vibrational frequencies calculated in localized coordinates," J. Chem. Phys. 143(16), 164104 (2015).
- ⁸¹ M. W. D. Hanson-Heine, "Intermediate vibrational coordinate localization with harmonic coupling constraints," J. Chem. Phys. 144(20), 204116 (2016).
- ⁸²G. Rauhut and B. Hartke, "Modeling of high-order many-mode terms in the expansion of multidimensional potential energy surfaces: Application to vibrational spectra," J. Chem. Phys. 131(1), 014108 (2009).
- ⁸³ B. Ziegler and G. Rauhut, "Localized normal coordinates in accurate vibrational structure calculations: Benchmarks for small molecules," J. Chem. Theory Comput. 15(7), 4187–4196 (2019).
- ⁸⁴G. M. J. Barca, C. Bertoni, L. Carrington, D. Datta, N. De Silva, J. E. Deustua, D. G. Fedorov, J. R. Gour, A. O. Gunina, E. Guidez, T. Harville, S. Irle, J. Ivanic, K. Kowalski, S. S. Leang, H. Li, W. Li, J. J. Lutz, I. Magoulas, J. Mato, V. Mironov, H. Nakata, B. Q. Pham, P. Piecuch, D. Poole, S. R. Pruitt, A. P. Rendell, L. B. Roskop, K. Ruedenberg, T. Sattasathuchana, M. W. Schmidt, J. Shen, L. Slipchenko, M. Sosonkina, V. Sundriyal, A. Tiwari, J. L. Galvez Vallejo, B. Westheimer, M. Włoch, P. Xu, F. Zahariev, and M. S. Gordon, "Recent developments in the general atomic and molecular electronic structure system," J. Chem. Phys. 152(15), 154102 (2020).
- ⁸⁵M. Majland, R. Berg Jensen, M. Greisen Højlund, N. Thomas Zinner, and O. Christiansen, "Optimizing the number of measurements for vibrational structure on quantum computers: Coordinates and measurement schemes," Chem. Sci. 14(28), 7733–7742 (2023).

- ⁸⁶R. M. Richard, K. U. Lao, and J. M. Herbert, "Approaching the complete-basis limit with a truncated many-body expansion," J. Chem. Phys. **139**(22), 224102 (2013).
- ⁸⁷R. M. Richard, K. U. Lao, and J. M. Herbert, "Aiming for benchmark accuracy with the many-body expansion," Acc. Chem. Res. 47(9), 2828–2836 (2014).
- ⁸⁸J. Mato, D. Tzeli, and S. S. Xantheas, "The many-body expansion for metals. I. The alkaline earth metals Be, Mg, and Ca," J. Chem. Phys. **157**(8), 084313 (2022).
- ⁸⁹ J. P. Heindel and S. S. Xantheas, "The many-body expansion for aqueous systems revisited: I. Water–Water interactions," J. Chem. Theory Comput. 16(11), 6843–6855 (2020).
- ⁹⁰ A. Hermann, R. P. Krawczyk, M. Lein, P. Schwerdtfeger, I. P. Hamilton, and J. J. P. Stewart, "Convergence of the many-body expansion of interaction potentials: From van der Waals to covalent and metallic systems," Phys. Rev. A 76(1), 013202 (2007).
- ⁹¹B. Paulus, K. Rosciszewski, N. Gaston, P. Schwerdtfeger, and H. Stoll, "Convergence of the *ab initio* many-body expansion for the cohesive energy of solid mercury," Phys. Rev. B **70**(16), 165106 (2004).
- ⁹²I. G. Kaplan, R. Santamaria, and O. Novaro, "Non-additive forces in atomic clusters," Mol. Phys. 84(1), 105–114 (1995).
- ⁹³T. W. Keal and D. J. Tozer, "Semiempirical hybrid functional with improved performance in an extensive chemical assessment," J. Chem. Phys. 123(12), 121103 (2005).
- ⁹⁴T. H. Dunning, Jr., "Gaussian basis sets for use in correlated molecular calculations. I. The atoms boron through neon and hydrogen," J. Chem. Phys. **90**(2), 1007–1023 (1989).
- ⁹⁵S. Dasgupta and J. M. Herbert, "Standard grids for high-precision integration of modern density functionals: SG-2 and SG-3," J. Comput. Chem. 38(12), 869–882 (2017).
- ⁹⁶C. König and O. Christiansen, "Linear-scaling generation of potential energy surfaces using a double incremental expansion," J. Chem. Phys. **145**(6), 064105 (2016).
- ⁹⁷K. Pflüger, M. Paulus, S. Jagiella, T. Burkert, and G. Rauhut, "Multi-level vibrational SCF calculations and ftir measurements on furazan," Theor. Chem. Acc. 114(4–5), 327–332 (2005).
- ⁹⁸ J. A. Tan and J.-L. Kuo, "Multilevel approach for Direct VSCF/VCI multimode calculations with applications to large 'Zundel' cations," J. Chem. Theory Comput. 14(12), 6405–6416 (2018).
- ⁹⁹C. König, "Tailored multilevel approaches in vibrational structure theory: A route to quantum mechanical vibrational spectra for complex systems," Int. J. Quantum Chem. 121(3), e26375 (2021).
- ¹⁰⁰K. Yagi, S. Hirata, and K. Hirao, "Multiresolution potential energy surfaces for vibrational state calculations," Theor. Chem. Acc. 118(3), 681–691 (2007).
- ¹⁰¹V. Babin, C. Leforestier, and F. Paesani, "Development of a 'first principles' water potential with flexible monomers: Dimer potential energy surface, VRT spectrum, and second virial coefficient," J. Chem. Theory Comput. 9(12), 5395–5403 (2013).
- ¹⁰²V. Babin, G. R. Medders, and F. Paesani, "Development of a 'first principles' water potential with flexible monomers. II: Trimer potential energy surface, third virial coefficient, and small clusters," J. Chem. Theory Comput. 10(4), 1599–1607 (2014).
- ¹⁰³G. R. Medders, V. Babin, and F. Paesani, "Development of a 'first-principles' water potential with flexible monomers. III. Liquid phase properties," J. Chem. Theory Comput. 10(8), 2906–2910 (2014).
- ¹⁰⁴G. R. Medders and F. Paesani, "Infrared and Raman spectroscopy of liquid water through 'first-principles' many-body molecular dynamics," J. Chem. Theory Comput. 11(3), 1145–1154 (2015).
- ¹⁰⁵ E. Epifanovsky, A. T. B. Gilbert, X. Feng, J. Lee, Y. Mao, N. Mardirossian, P. Pokhilko, A. F. White, M. P. Coons, A. L. Dempwolff, Z. Gan, D. Hait, P. R. Horn, L. D. Jacobson, I. Kaliman, J. Kussmann, A. W. Lange, K. U. Lao, D. S. Levine, J. Liu, S. C. McKenzie, A. F. Morrison, K. D. Nanda, F. Plasser, D. R. Rehn, M. L. Vidal, Z.-Q. You, Y. Zhu, B. Alam, B. J. Albrecht, A. Aldossary, E. Alguire, J. H. Andersen, V. Athavale, D. Barton, K. Begam, A. Behn, N. Bellonzi, Y. A. Bernard, E. J. Berquist, H. G. A. Burton, A. Carreras, K. Carter-Fenk, R. Chakraborty, A. D. Chien, K. D. Closser, V. Cofer-Shabica, S. Dasgupta, M. de Wergifosse, J. Deng, M. Diedenhofen, H. Do, S. Ehlert, P.-T. Fang, S. Fatehi, Q. Feng, T. Friedhoff, J. Gayvert, Q. Ge, G. Gidofalvi, M. Goldey, J. Gomes, C. E. González-Espinoza, S.

Gulania, A. O. Gunina, M. W. D. Hanson-Heine, P. H. P. Harbach, A. Hauser, M. F. Herbst, M. Hernández Vera, M. Hodecker, Z. C. Holden, S. Houck, X. Huang, K. Hui, B. C. Huynh, M. Ivanov, Á. Jász, H. Ji, H. Jiang, B. Kaduk, S. Kähler, K. Khistyaev, J. Kim, G. Kis, P. Klunzinger, Z. Koczor-Benda, J. H. Koh, D. Kosenkov, L. Koulias, T. Kowalczyk, C. M. Krauter, K. Kue, A. Kunitsa, T. Kus, I. Ladjánszki, A. Landau, K. V. Lawler, D. Lefrancois, S. Lehtola, R. R. Li, Y.-P. Li, J. Liang, M. Liebenthal, H.-H. Lin, Y.-S. Lin, F. Liu, K.-Y. Liu, M. Loipersberger, A. Luenser, A. Manjanath, P. Manohar, E. Mansoor, S. F. Manzer, S.-P. Mao, A. V. Marenich, T. Markovich, S. Mason, S. A. Maurer, P. F. McLaughlin, M. F. S. J. Menger, J.-M. Mewes, S. A. Mewes, P. Morgante, J. W. Mullinax, K. J. Oosterbaan, G. Paran, A. C. Paul, S. K. Paul, F. Pavošević, Z. Pei, S. Prager, E. I. Proynov, Á. Rák, E. Ramos-Cordoba, B. Rana, A. E. Rask, A. Rettig, R. M. Richard, F. Rob, E. Rossomme, T. Scheele, M. Scheurer, M. Schneider, N. Sergueev, S. M. Sharada, W. Skomorowski, D. W. Small, C. J. Stein, Y.-C. Su, E. J. Sundstrom, Z. Tao, J. Thirman, G. J. Tornai, T. Tsuchimochi, N. M. Tubman, S. P. Veccham, O. Vydrov, J. Wenzel, J. Witte, A. Yamada, K. Yao, S. Yeganeh, S. R. Yost, A. Zech, I. Y. Zhang, X. Zhang, Y. Zhang, D. Zuev, A. Aspuru-Guzik, A. T. Bell, N. A. Besley, K. B. Bravaya, B. R. Brooks, D. Casanova, J.-D. Chai, S. Coriani, C. J. Cramer, G. Cserey, A. E. DePrince, R. A. DiStasio, A. Dreuw, B. D. Dunietz, T. R. Furlani, W. A. Goddard, S. Hammes-Schiffer, T. Head-Gordon, W. J. Hehre, C.-P. Hsu, T.-C. Jagau, Y. Jung, A. Klamt, J. Kong, D. S. Lambrecht, W. Liang, N. J. Mayhall, C. W. McCurdy, J. B. Neaton, C. Ochsenfeld, J. A. Parkhill, R. Peverati, V. A. Rassolov, Y. Shao, L. V. Slipchenko, T. Stauch, R. P. Steele, J. E. Subotnik, A. J. W. Thom, A. Tkatchenko, D. G. Truhlar, T. Van Voorhis, T. A. Wesolowski, K. B. Whaley, H. L. Woodcock, P. M. Zimmerman, S. Faraji, P. M. W. Gill, M. Head-Gordon, J. M. Herbert, and A. I. Krylov, "Software for the frontiers of quantum chemistry: An overview of developments in the Q-chem 5 package," J. Chem. Phys. 155(8), 084801 (2021).

¹⁰⁶X. Cheng and R. P. Steele, "Efficient anharmonic vibrational spectroscopy for large molecules using local-mode coordinates," J. Chem. Phys. **141**(10), 104105 (2014).

- ¹⁰⁷X. Cheng, J. J. Talbot, and R. P. Steele, "Tuning vibrational mode localization with frequency windowing," J. Chem. Phys. **145**(12), 124112 (2016).
- ¹⁰⁸R. T. Pack, "Coordinates for an optimum Cs approximation in reactive scattering," Chem. Phys. Lett. **108**(4), 333–338 (1984).
- ¹⁰⁹R. T. Pack and G. A. Parker, "Quantum reactive scattering in three dimensions using hyperspherical (APH) coordinates. Theory," J. Chem. Phys. 87(7), 3888–3921 (1987).
- ¹¹⁰B. R. Johnson, "On hyperspherical coordinates and mapping the internal configurations of a three body system," J. Chem. Phys. 73(10), 005051–5058 (2008).
- ¹¹¹B. R. Johnson, "The quantum dynamics of three particles in hyperspherical coordinates," J. Chem. Phys. **79**(4), 1916–1925 (1983).
- ¹¹²F. Richter, P. Carbonniere, A. Dargelos, and C. Pouchan, "An adaptive potential energy surface generation method using curvilinear valence coordinates," J. Chem. Phys. 136(22), 224105 (2012).
- ¹¹³E. L. Klinting, D. Lauvergnat, and O. Christiansen, "Vibrational coupled cluster computations in polyspherical coordinates with the exact analytical kinetic energy operator," J. Chem. Theory Comput. 16(7), 4505–4520 (2020).
- ¹¹⁴K. Yagi, K. Hirao, T. Taketsugu, M. W. Schmidt, and M. S. Gordon, "Ab initio vibrational state calculations with a quartic force field: Applications to H₂CO, C₂H₄, CH₃OH, CH₃CCH, and C₆H₆," J. Chem. Phys. **121**(3), 1383–1389 (2004).
- ¹¹⁵C. R. Jacob and M. Reiher, "Localizing normal modes in large molecules," J. Chem. Phys. **130**(8), 084106 (2009).
- ¹¹⁶M. W. D. Hanson-Heine, "Reduced basis set dependence in anharmonic frequency calculations involving localized coordinates," J. Chem. Theory Comput. 14(3), 1277–1285 (2018).
- ¹¹⁷D. Peláez and H.-D. Meyer, "The multigrid potfit (MGPF) method: Grid representations of potentials for quantum dynamics of large systems," J. Chem. Phys. 138(1), 014108 (2013).